

High-pressure phases of silane

Chris J. Pickard and R. J. Needs

*Theory of Condensed Matter Group, Cavendish Laboratory,
J. J. Thomson Avenue, Cambridge CB3 0HE, United Kingdom*

(Dated: February 6, 2008)

It has been suggested that hydrogen may metallise at lower pressures if it is “precompressed”. Here we introduce a search strategy for predicting high-pressure structures and apply it to silane using first-principles electronic structure computations. It is based on relaxing randomly chosen structures, and is demonstrated to work well for unit cells containing up to at least ten atoms. We predict that silane will metallise at higher pressures than previously anticipated, but we suggest that the metallic phase might show high-temperature superconductivity at experimentally accessible pressures.

PACS numbers: 61.66.Fn, 71.20.-b, 74.10.+v

As early as 1935 Wigner and Huntingdon suggested that hydrogen would become metallic under sufficient compression.[1] There have been many attempts to produce metallic hydrogen under high-pressure laboratory conditions, but it has stubbornly remained insulating in diamond-anvil-cell experiments up to the highest pressure so far achieved of 342 GPa.[2] It has recently been suggested[3] that the group IV hydrides, methane (CH_4), silane (SiH_4), and germane (GeH_4), might become metallic at pressures achievable in diamond anvil cells because the hydrogen in these materials is “chemically precompressed” by the presence of the group IV atoms. Such metallic phases might exhibit phonon-mediated high-temperature superconductivity.

Recently, Feng *et al.*[4] reported a first-principles density-functional-theory (DFT) study of silane at high pressures. They predicted that a layered structure would be stable at pressures above 25 GPa. This phase was found to be semi-metallic at 91 GPa, and the density of electronic states at the Fermi energy increased rapidly with further application of pressure. An estimate using the Bardeen-Cooper-Schrieffer (BCS) theory [5] indicated that the superconducting transition temperature would increase from about 0 K at 91 GPa to about 166 K at 202 GPa, pressures which are comfortably within range of diamond anvil cells.

Accurate cohesive energies and equilibrium volumes for materials of known crystal structure have been obtained using first-principles methods, but the prediction of stable structures has remained very difficult. Using these methods, it is routine to relax a structure from a chosen initial configuration to a nearby minimum in the potential energy surface. Relaxing from a set of initial configurations may lead to several distinct local-energy minima, the lowest-energy one corresponding to the most favoured structure. However, if none of the initial configurations is sufficiently close to the global minimum then the configurations will become trapped in higher-energy local minima. Trapping in local-energy minima is a severe problem because the number of minima is

expected to increase exponentially with the number of degrees of freedom. In the past this problem has typically been addressed by selecting initial configurations derived from experimental information known about the system in question, the known structures of similar materials, chemical intuition, and results from simpler computational methods. The shortcomings in this approach have led to a growth in using first-principles methods in combination with more advanced search techniques to determine stable structures.[6, 7, 8, 9]

We have developed a simple strategy for generating initial configurations, which consists of choosing essentially random unit cell parameters and atomic positions. We first choose the number and identity of the atoms in the unit cell. To form “random” unit cells we choose three cell-vector lengths randomly and uniformly between 0.5 and 1.5 (in arbitrary units), and three cell angles randomly and uniformly between 40° and 140° . The resulting cell vectors are scaled to produce the desired volume, which is also selected randomly and uniformly from between 0.5 and 1.5 of some chosen volume. The positions of the atoms are then chosen randomly and uniformly within the cell. First-principles methods are then used to relax each structure until a minimum in the enthalpy is reached. The structures obtained from such a procedure are clearly liable to be trapped in local minima, and undoubtedly the probability of finding the global minimum will drop rapidly with increasing complexity of the system. However, for systems of moderate complexity, tests indicate that our approach has a high probability of locating the global minimum. In practice, the number of initial configurations required to find the global minimum depends on the system, and particularly on the number of degrees of freedom it possesses. Our approach has been to continue generating configurations until the relaxed structures with low energies are generated several times and, where possible, to look for the occurrence of previously-known “marker” structures.

All of the first-principles calculations were performed using a developer’s version of the CASTEP code.[10] For

the initial search over structures we used the local density approximation (LDA) for the exchange-correlation functional[11], and default ultrasoft pseudopotentials.[12] The k -point sets were generated separately for each unit cell encountered during the procedure, and no symmetry restrictions were applied at any point. Medium quality Brillouin zone sampling using a grid of spacing $2\pi \times 0.07 \text{ \AA}^{-1}$ and a plane wave basis set cutoff of 280 eV were found to be sufficient for the initial search over structures. When re-calculating the enthalpy curves with higher accuracy we used a Brillouin zone sampling of $2\pi \times 0.03 \text{ \AA}^{-1}$, harder pseudopotentials requiring a plane wave cutoff of 360 eV, and the Perdew-Burke-Ernzerhof (PBE) Generalised Gradient Approximation (GGA) density functional[13] to aid comparison with Ref. [4]. Each of the calculations was for the zero-temperature ground state and we neglected the zero-point vibrational energy.

We have applied our approach to silicon at zero pressure. Using two-atom unit cells and 100 randomly chosen initial configurations, we obtained the global minimum energy diamond structure (15 times), β -tin (2 times), Imma (14 times), and simple hexagonal (15 times). Both experiment and DFT calculations agree that these phases are the four lowest-pressure thermodynamically stable phases of silicon.[14] A study of 8-atom unit cells of carbon at 300 GPa generated the diamond structure as the lowest-enthalpy phase in addition to numerous higher-enthalpy phases, including the BC8 phase, which has been postulated as a stable phase of carbon at TPa pressures.[16] We also studied 16-atom unit cells of hydrogen at 250 GPa, finding, among other phases, the *Cmca* molecular phase which DFT calculations have predicted to be the most stable at that pressure.[17]

Our approach is particularly suitable for the prediction of the structures of high-pressure phases because they often have fairly simple structures with a small number of atoms in the primitive unit cell. In addition, our method is straightforward and does not require the selection of highly-system-specific parameter values. Our scheme could be modified to include other features, such as methods for extricating configurations from local energy minima.[18] However, such modifications would complicate the method and add to the computational cost, which would limit the number of initial configurations which can be sampled. It is also possible to introduce other constraints on the initial configurations so that one can predict the structures of clusters, defects, surfaces, etc. For example, we have used our approach to search for low-energy self-interstitial defect structures in silicon. To construct the initial configurations we took a 32-atom body-centred-cubic unit cell of diamond-structure silicon, removed an atom and its four nearest neighbours, and then placed six silicon atoms randomly within a spherical region of radius about 1.5 bond lengths centred on the first atom that we removed. Using our approach, we readily found the split- $\langle 110 \rangle$ and

hexagonal interstitial configurations, which other DFT calculations have shown to be lowest in energy[19], and also predicted that all other self-interstitial local energy minima are at least 0.3 eV higher in energy. The generation of numerous low-energy structures is an interesting and useful feature of our strategy, as they can give information about the structures which might be formed under other conditions of pressure and temperature, or out of thermal equilibrium.

We tested our search strategy for simulation cells containing one, two, and four SiH_4 units at a pressure of 250 GPa. With one SiH_4 unit per cell the lowest-enthalpy structure occurred four times from 13 initial configurations, but it was 0.36 eV per SiH_4 unit higher in enthalpy than the most stable structure found with two SiH_4 units per cell, which occurred 8 times from 37 initial configurations. With four SiH_4 units per cell the most stable structure was 0.13 eV per SiH_4 unit higher in enthalpy than for the two SiH_4 unit cell, and each of the low-enthalpy phases occurred only once from 38 configurations. Clearly the simulation cells containing one SiH_4 unit are too constrained to produce very-low-enthalpy structures, while those containing four SiH_4 units have too many degrees of freedom for our search strategy to find the global minimum enthalpy structure with the number of initial configurations used. We concluded that using two SiH_4 units per simulation cell and 40 initial configurations represented an affordable and efficient approach to finding low-enthalpy phases of silane at high pressures.

Further runs were performed at 0, 50, 100, 150, and 200 GPa, with two SiH_4 units per simulation cell and 40 initial structures. At 0 GPa the lowest-energy structure could not be determined with confidence because the low-energy structures were not found repeatedly. This reflects the fact that at zero pressure many different structures have similar energies (within 0.1 eV per SiH_4 unit), including those consisting of silane molecules, disilane plus a hydrogen molecule, and various polymeric forms plus hydrogen molecules. The various packings of silane molecules were therefore inadequately explored using just 40 initial structures. The lowest-energy structure found (by about 40 meV per SiH_4 unit) was a low-symmetry silane molecular crystal which was about 50 meV per SiH_4 unit less stable than the higher-symmetry T1 packing considered by Feng *et al.* [4].

Having selected the low-enthalpy phases from the above runs, we re-calculated their enthalpies with greater computational accuracy. The calculated enthalpies of various structures are shown as a function of pressure in Fig. 1. The details of some of the lower-enthalpy structures found are described in the auxiliary material to this Letter.[15]

An insulating chain-like structure with $P2/c$ symmetry was found to be the most stable in a small region of pressures around 40 GPa, but a structure of $I4_1/a$ sym-

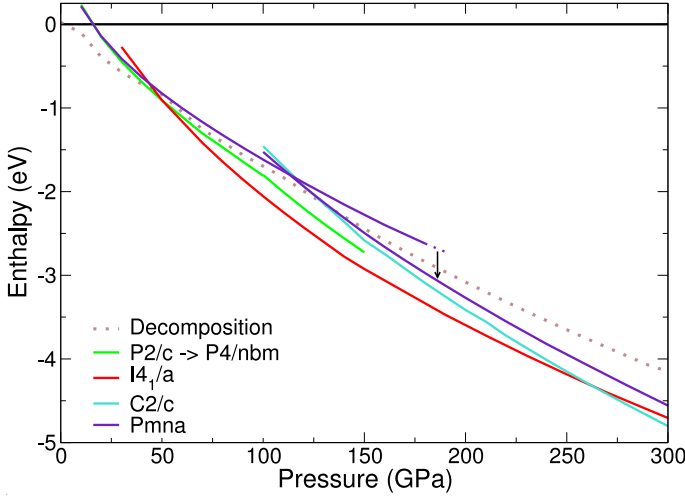


FIG. 1: The enthalpies per SiH_4 unit of various structures as a function of pressure, referenced to the T1 phase of Ref. [4].

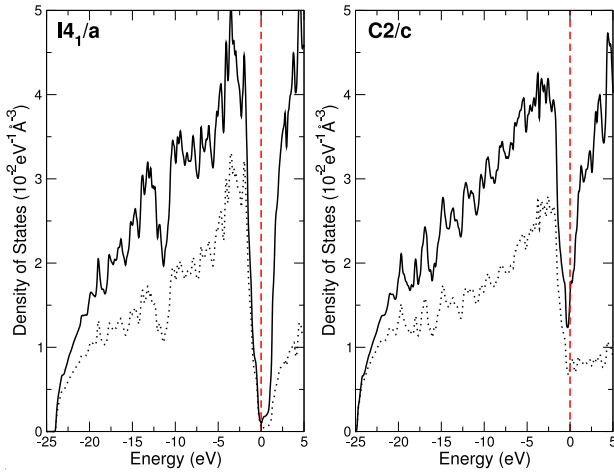


FIG. 2: The densities of states of the $I4_1/a$ and $C2/c$ phases at their predicted coexistence pressure of 262.5 GPa. The partial density of states projected onto the H atoms is shown by dashed curves, and the Fermi energies are indicated by the vertical dashed lines.

metry became more stable at about 50 GPa. The $I4_1/a$ phase is predicted to be insulating at 50 GPa but, as the pressure is increased, the bandgap gradually closes and it becomes semi-metallic, as can be seen in the density of states plotted in Fig. 2. Given the well-known shortcomings of standard DFT approaches such as the LDA and GGA functionals, which normally underestimate band gaps, it is likely that our calculations underestimate the pressure at which the $I4_1/a$ phase becomes semi-metallic. The $I4_1/a$ phase remains the lowest-enthalpy phase up to 262.5 GPa, at which pressure a denser structure of $C2/c$ symmetry becomes stable. This phase is a good metal, see Fig. 2.

In the $I4_1/a$ structure, which is illustrated in Fig. 3, each Si atom is bonded to 8 H atoms. Each of the

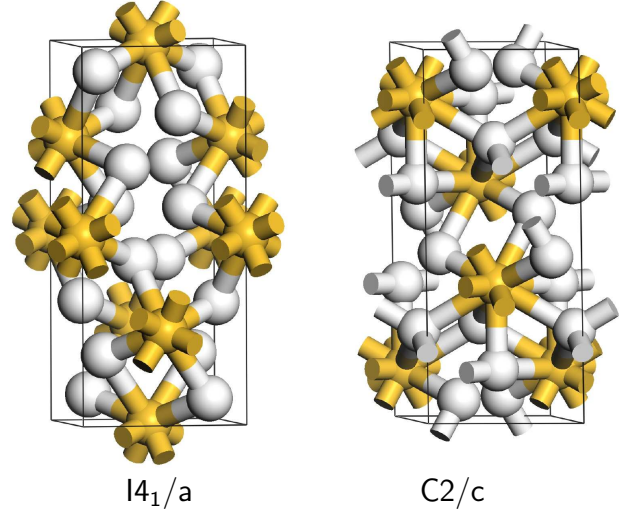


FIG. 3: The $I4_1/a$ and $C2/c$ structures. The golden spheres represent silicon atoms, and the white spheres hydrogen. Note the Si_2H_2 planes in the $I4_1/a$ structure, and the two, three and four-fold coordinated H atoms in the $C2/c$ structure.

H atoms forms a “bridge” between two neighbouring Si atoms. There are two such bridges between every pair of neighbouring Si atoms, the four atoms forming a Si_2H_2 plane. This bonding arrangement consists of two “banana bonds”, which are electron-deficient three-centre-two-electron bonds, reminiscent of those in B_2H_6 (diborane).[20] The arrangement of the Si_2H_2 planes keeps the H atoms away from each other, and the $I4_1/a$ structure contains only Si-H bonds. Each of the Si sites and the H sites is equivalent in this high-symmetry structure which has a 10-atom primitive unit cell. The layered O3 structure proposed in Ref. [4] also contains some bridging Si-H-Si bonds, although it also contains H atoms which are bonded to single Si atoms. Our $I4_1/a$ structure is about 0.4 eV per SiH_4 unit lower in enthalpy than the O3 structure at 100 GPa, and about 0.7 eV per SiH_4 unit lower at 180 GPa.

In the metallic $C2/c$ structure illustrated in Fig. 3, each Si atom is bonded to 11 H atoms. Each of the Si sites is equivalent and there are three inequivalent H sites in which the H atom forms bonds to two, three, or four Si atoms. The average coordination number of the H atoms in the $C2/c$ structure is larger than in $I4_1/a$, which accounts for its smaller equilibrium volume. The metallic character of this phase means that the nature of the inter-atomic bonding is less clear cut than in the $I4_1/a$ structure, but again a description in terms of electron deficient Si-H bonds is appropriate.

Our search also revealed a number of other low-enthalpy phases, including the O3 $Pmna$ structure studied by Feng *et al.*[4] We found that, at around 200 GPa, O3 $Pmna$ converts into a more compressed structure of the same symmetry, but it still has a substantially higher

enthalpy than our $I4_1/a$ phase. We followed the more compressed phase to lower pressures and found it to be more stable than the O3 $Pmna$ structure down to about 110 GPa. We also found a low-enthalpy phase with $I\bar{4}2d$ symmetry which is only 0.1 eV per SiH_4 unit above the most stable phase at 100 GPa. The $P2/c$ phase mentioned above converts to a structure with $P4/nbm$ symmetry at 100 GPa. Interestingly, the $P4/nbm$ phase has a layered structure, like the O3 structure, but with every hydrogen atom participating in a bridging bond, which results in its lower enthalpy.

Having found the low-enthalpy metallic $C2/c$ structure using simulation cells containing two SiH_4 units, we studied its stability to rearrangements of the H atoms using simulation cells containing four SiH_4 units at 250 GPa. To make initial configurations we used the $C2/c$ Si framework and placed the 16 H atoms randomly within the simulation cell, and then relaxed all of the atomic positions and cell parameters. Using 15 such initial configurations we obtained the $C2/c$ structure as the lowest-enthalpy phase, an $Fddd$ structure only 30 meV per SiH_4 unit higher in enthalpy, and several other slightly less stable phases. All of the low-enthalpy phases contained a mixture of two-, three-, and four-fold coordinated H atoms, as in the $C2/c$ structure, and they all had very similar volumes and densities of electronic states.

Silane is in fact unstable to decomposition into hydrogen and silicon at zero pressure, and we therefore considered the thermodynamic stability of our new silane phases against processes involving the formation of hydrogen molecules. At low pressures we found some low-enthalpy structures containing covalently bonded hydrogen molecules, indicating the instability of silane at these pressures, but none of the low-enthalpy structures at high pressures contain any H-H bonds, suggesting stability against decomposition. We investigated this further by considering decomposition into diamond-structure Si and molecular hydrogen at zero pressure, into simple hexagonal silicon[14] and $Cmca$ -structure hydrogen[17] phases up to 40 GPa, and into face-centred cubic silicon and $Cmca$ -structure hydrogen at higher pressures. While the O3 structure proposed in Ref. [4] is found to be unstable with respect to decomposition into face-centred cubic silicon and $Cmca$ -structure hydrogen at its metallization pressure, our $I4_1/a$ and $C2/c$ structures are stable with respect to such a decomposition. This lends further weight to our contention that the $C2/c$ structure of silane, or something very like it, is thermodynamically stable at high pressures.

We now discuss the possibility of phonon-mediated superconductivity in the $C2/c$ phase. Within the BCS theory, the superconducting transition temperature depends on the values of three parameters: the density of states at the Fermi energy of the normal state, the Debye temperature of the phonons, and the effective electron-phonon coupling parameter. We estimated the densities

of states at the Fermi energies of the $C2/c$ and $I4_1/a$ phases at their coexistence pressure of 262.5 GPa using DFT methods. As shown in Fig. 2, the $C2/c$ phase is a good metal, with a density of states at the Fermi energy of $1.6 \times 10^{-2} \text{ eV}^{-1} \text{ \AA}$, which is about 46% of the free-electron value and is close to the zero-pressure value for lead. We decomposed the densities of states into H- and Si-associated components using a Mulliken population analysis.[21] Fig. 2 shows that below the Fermi energy the density of states is a little larger on the H atoms than on the Si ones, while above the Fermi energy it becomes progressively larger on the Si atoms. This is consistent with the fact that the Pauling electronegativity of H (2.2) is a little larger than that of Si (1.9). The fact that the density of electronic states at the Fermi energy projected onto the H atoms is large suggests that the coupling between the electrons close to the Fermi energy and phonon modes involving motions of the H atoms may be significant. We also performed DFT calculations of the Γ -point phonon frequencies of the $C2/c$ phase at 262.5 GPa, finding the highest phonon frequency to be 2500 cm^{-1} . This corresponds to an estimated Debye temperature of 3600 K, which is about 40 times larger than that of lead at zero-pressure. An examination of the phonon eigenvectors indicates that the highest-frequency modes correspond largely to motions of the H atoms. The very large Debye temperature and the substantial density of states at the Fermi energy suggests that the $C2/c$ phase might exhibit high-temperature superconductivity, but one should be cautious about this conclusion. A reliable estimate of the superconducting transition temperature within the BCS theory also requires evaluation of the full electron-phonon coupling matrix elements, which is beyond the scope of this work.

In summary, we have used a random searching strategy in conjunction with first-principles electronic structure computations to predict the stable high-pressure phases of silane. We find insulating/semi-metallic behaviour up to 260 GPa, at which point a first-order phase transition occurs to a good metal. This phase might show high-temperature superconductivity at a pressure which is achievable within a diamond anvil cell.

CJP was supported by an EPSRC Advanced Research Fellowship. We thank Peter Littlewood for useful discussions, and Keith Refson for assistance in performing the phonon calculations.

-
- [1] E. Wigner and H. B. Huntington, J. Chem. Phys. **3**, 764 (1935).
 - [2] C. Narayana, H. Luo, J. Orloff, and A. L. Ruoff, Nature **393**, 46 (1998).
 - [3] N. W. Ashcroft, Phys. Rev. Lett. **92**, 187002 (2004).
 - [4] J. Feng, W. Grochala, T. Jaron, R. Hoffmann, A. Bergara, and N. W. Ashcroft, Phys. Rev. Lett. **96**,

Pressure (GPa)	Space group	Lattice parameters (Å, °)			Atomic coordinates (fractional)			
50	$P2/c$	$a=4.70$	$b=4.02$	$c=3.48$	Si	0.5000	0.2078	0.7500
		$\alpha=90.00$	$\beta=137.34$	$\gamma=90.00$	H1	0.7745	0.1272	0.6642
					H2	0.1919	0.4024	0.2277
100	$I\bar{4}2d$	$a=4.26$	$b=4.26$	$c=3.95$	Si	0.0000	0.0000	0.0000
		$\alpha=90.00$	$\beta=90.00$	$\gamma=90.00$	H	0.3285	0.0367	0.1195
150	$P4/nbm$	$a=3.35$	$b=3.35$	$c=2.80$	Si	0.5000	0.5000	0.5000
		$\alpha=90.00$	$\beta=90.00$	$\gamma=90.00$	H	0.3553	0.0367	0.1195
150	$I4_1/a$	$a=3.04$	$b=3.04$	$c=6.85$	Si	0.5000	0.5000	0.5000
		$\alpha=90.00$	$\beta=90.00$	$\gamma=90.00$	H	0.8676	0.2166	0.4328
250	$C2/c$	$a=2.94$	$b=6.79$	$c=2.90$	Si	0.5000	0.6334	0.2500
		$\alpha=90.00$	$\beta=115.20$	$\gamma=90.00$	H1	0.8028	0.4462	0.4986
					H2	0.0000	0.6389	0.7500
					H3	0.0000	0.7549	0.2500

TABLE I: Details of some of the structures produced by the search. The structures have been optimised at the higher level of accuracy described in the letter. Only the fractional coordinates of symmetry inequivalent atoms are reported.

- 017006 (2006).
- [5] J. Bardeen, L. N. Cooper, and J. R. Schrieffer, Phys. Rev. **108**, 1175 (1957).
- [6] R. Martonak, A. Laio, and M. Parrinello, Phys. Rev. Lett. **90**, 075503 (2003).
- [7] S. Yoo and X. C. Zeng, Angewandte Chemie International Edition **44**, 1491 (2005).
- [8] S. Goedecker, W. Hellmann, and T. Lenosky, Phys. Rev. Lett. **95**, 055501 (2005).
- [9] A. R. Oganov, C. W. Glass, and S. Ono, Earth and Planetary Science Letters **241**, 95 (2006).
- [10] M. D. Segall, P. J. D. Lindan, M. J. Probert, C. J. Pickard, P. J. Hasnip, S. J. Clark, and M. C. Payne, J. Phys: Condens. Matter **14**, 2717 (2002).
- [11] J. P. Perdew and A. Zunger, Phys. Rev. B **23**, 5048 (1981).
- [12] D. Vanderbilt, Phys. Rev. B **41**, 7892 (1990).
- [13] J. P. Perdew, K. Burke, and M. Ernzerhof, Phys. Rev. Lett. **77**, 3865 (1996).
- [14] A. Mujica, A. Rubio, A. Muñoz, and R. J. Needs, Rev. Mod. Phys. **75**, 863 (2003).
- [15] See EPAPS document No. xxxxxxxxxxxx.
- [16] M. T. Yin, Phys. Rev. B **30**, 1773 (1984).
- [17] K. A. Johnson and N. W. Ashcroft, Nature **403**, 632 (2000).
- [18] D. J. Wales, *Energy Landscapes* (Cambridge University Press, 2003), chap. 6.
- [19] R. J. Needs, J. Phys: Condens. Matter **11**, 10437 (1999).
- [20] L. Burnelle and J. J. Kaufmann, J. Chem. Phys. **43**, 3540 (1965).
- [21] M. D. Segall, R. Shah, C. J. Pickard, and M. C. Payne, Phys. Rev. B **54**, 16317 (1996).